Eur. Phys. J. C 49, 293–296 (2007)
DOI 10.1140/epjc/s10052-006-0102-9

THE EUROPEAN PHYSICAL JOURNAL C

Regular Article – Experimental Physics

Energy dependence of proton and antiproton production in central Pb+Pb collisions from NA49

E. Kornas[a] for the NA49 Collaboration

Institute of Nuclear Physics PAN, Ul. Radzikowskiego 152, 31342 Krakow, Poland

Received: 3 August 2006 /
Published online: 28 November 2006 –

Abstract. Recent results of the NA49 collaboration on the production of p and $\overline{p}$ at midrapidity in central Pb+Pb collisions in the beam energy range 20–158 A GeV are presented. The preliminary results for the rapidity distributions of p and $\overline{p}$ at 40 A GeV are also discussed.

PACS. 25.75.Dw

1 Introduction

The study of heavy-ion collisions at relativistic energies allows to learn how baryon number, carried by nucleons, is distributed in the produced final state. One can obtain significant information about energy loss of colliding nuclei by exploring the rapidity dependence of p and $\overline{p}$ production.

The measurement of baryon stopping in heavy ion collisions provides essential information on the particle production mechanisms.

In Fig. 1, published by the BRAHMS collaboration [1], the net proton distributions measured at AGS, SPS and RHIC [1–5] are shown. The shape of these distributions depends strongly on energy. As seen, at AGS energies the net proton distribution peaks at midrapidity, while at the top SPS energy ($\sqrt{s_{NN}} = 17\,\mathrm{GeV}$) the distribution develops a minimum at midrapidity. This means that at SPS energies collisions exhibit larger transparency.

At RHIC ($\sqrt{s_{NN}} = 200\,\mathrm{GeV}$) the data follow this pattern and the distribution is flat over ± 1 unit around midrapidity and rises at rapidity interval $y = 2 - 3$. The midrapidity region at RHIC is not yet totally baryon free, however a transition from a baryon dominated system at lower energies to a mainly meson dominated system at RHIC can be observed.

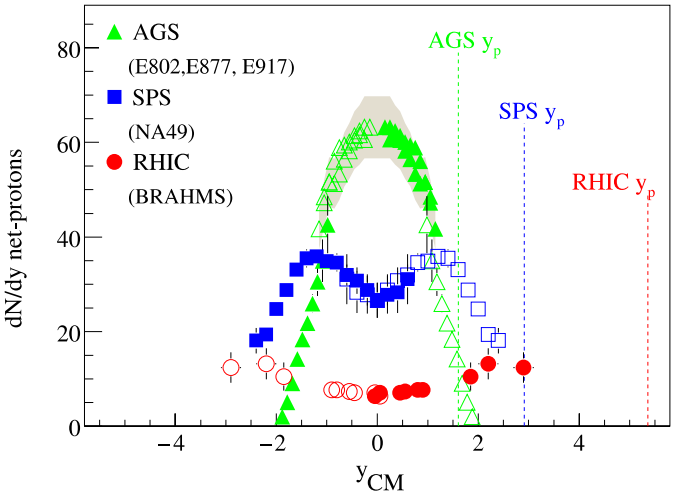

Fig. 1. The net proton rapidity distribution measured at AGS ($\sqrt{s_{NN}} = 5.5\,\mathrm{GeV}$), SPS ($\sqrt{s_{NN}} = 17\,\mathrm{GeV}$) and RHIC ($\sqrt{s_{NN}} = 200\,\mathrm{GeV}$) for 5% most central collisions. For RHIC data the *closed symbols* indicate measured points and *open symbols* are symmetrized, while the opposite is true for AGS and SPS data

2 The NA49 experiment

The NA49 detector [6], shown in Fig. 2, is a large acceptance fixed target hadron spectrometer at the CERN-SPS. The main tracking devices are four large volume time projection chambers (TPCs). Two of them, the Vertex TPCs (VTPC), are located in the magnetic field of two superconducting dipole magnets. The other two, Main TPCs (MTPC), are optimized for precise measurement of the ionization energy loss $\mathrm{d}E/\mathrm{d}x$ with a resolution 3%–6%.

The particle identification capability of the MTPCs is augmented at midrapidity by two Time of Flight (TOF) detectors (resolution 60 ps).

The centrality of the collisions is determined by a Veto Calorimeter (VCAL),which measures the energy carried by the projectile spectator nucleons. The NA49 experiment collected data in Pb+Pb collisions at beam energies between 20 A and 158 A GeV.

[a] e-mail: Ewelina.Kornas@ifj.edu.pl

3 Results

3.1 p and $\overline{p}$ production at midrapidity

At midrapidity both $\mathrm{d}E/\mathrm{d}x$ and TOF measurements are available and provide excellent particle identification.

Transverse mass distributions for protons and antiprotons for central Pb+Pb collisions at five SPS energies are shown in Fig. 3. The shape of m_t spectra hardly changes in the SPS energy region and can be described by hydro inspired models.

Figure 4 shows $\overline{p}/p$ ratio at midrapidity as a function of energy in central collisions at AGS, SPS and RHIC. The increase of the $\overline{p}/p$ ratio reflects the decrease of the baryochemical potential towards the higher energy.

Table 1 shows p and $\overline{p}$ yields at midrapidity at five beam energies. The midrapidity p yield decreases gradually with increasing energy in contrast to the rapidly rising $\overline{p}$ yield.

Details of the proton and antiproton analysis at midrapidity at SPS energies can be found in [7].

3.2 Rapidity spectra

The large acceptance of the NA49 detector allows measurements of rapidity spectra from midrapidity up to almost beam rapidity Due to the symmetry of Pb+Pb collisions

Table 1. Particle yield $\mathrm{d}n/\mathrm{d}y$ for protons and antiprotons at midrapidity in central Pb+Pb collisions at different beam energies

Energy (A GeV)	$\mathrm{d}n/\mathrm{d}y$ p	$\mathrm{d}n/\mathrm{d}y$ $\overline{p}$
20	46.1±2.1	0.06±0.01
30	42.1±2.0	0.16±0.02
40	41.3±1.1	0.32±0.03
80	30.1±1.0	0.87±0.07
158	29.6±0.9	1.66±0.17

4π yields can be determined. Raw p and $\overline{p}$ yields were extracted from fits of a sum of four Gaussian-like functions to the $\mathrm{d}E/\mathrm{d}x$ distributions in narrow bins of momentum and transverse momentum. They were corrected for geometrical acceptance and reconstruction efficiency, which is better that 98% in all bins. The track reconstruction efficiency was calculated by embedding simulated particle tracks into raw data events, which were then passed through the same reconstruction procedure as the real data. The final rapidity distributions were obtained by integration over the transverse momentum distribution in each y-bin. In Figs. 5 and 6 the preliminary rapidity distributions of protons and antiprotons measured in central Pb+Pb collisions at 40 A GeV are shown. The results have not yet been corrected for feed-down from weak decays, but the bias has

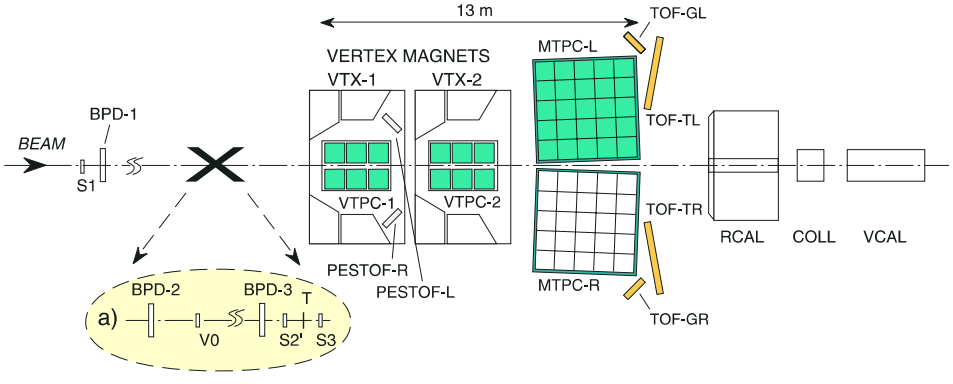

Fig. 2. The experimental set-up of the NA49 experiment

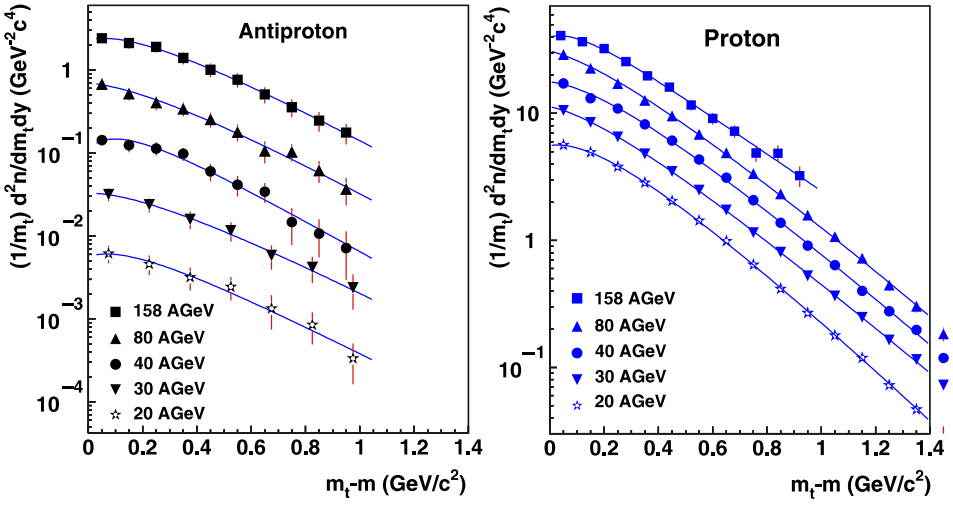

Fig. 3. Transverse mass distribution for antiprotons and protons at midrapidity in central Pb+Pb collisions at SPS energies. *Curves* show fits with a sum of two exponential functions [7]. For clarity, the spectra are scaled down by a factor of 2 successively from the uppermost data

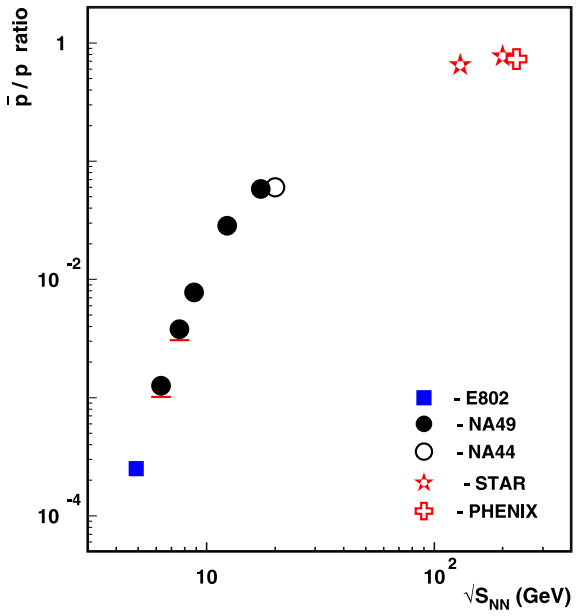

Fig. 4. The energy dependence of $\overline{p}/p$ ratio at midrapidity for central Pb+Pb/Au+Au reactions

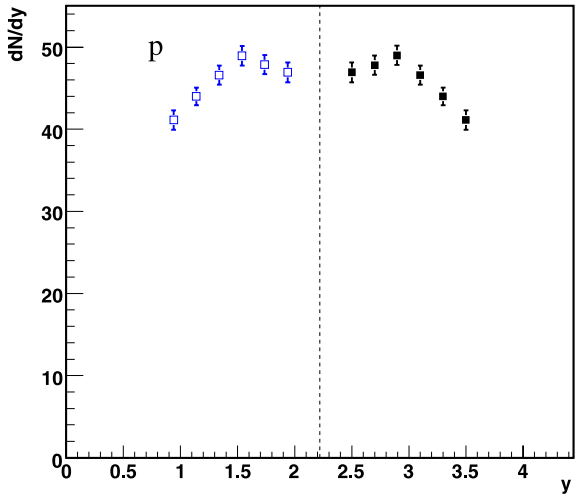

Fig. 5. Rapidity distribution of p in central Pb+Pb collisions at 40 A GeV. The *full symbols* indicate measured values, while the *open symbols* are reflected around midrapidity (*dotted line*)

been estimated to be about 18% for protons and 35% for antiprotons. It can be seen that the antiproton distribution peaks around midrapidity, while for protons there is a shallow minimum at midrapidity. Thus the net proton distribution at 40 A GeV, shown in Fig. 7, has a shape similar to the one at 158 A GeV ([2] and Fig. 1).

4 Summary and outlook

The midrapidity transverse mass distributions for protons and antiprotons at 20, 30, 40, 80 and 158 A GeV were shown. No visible change in the mean transverse mass for

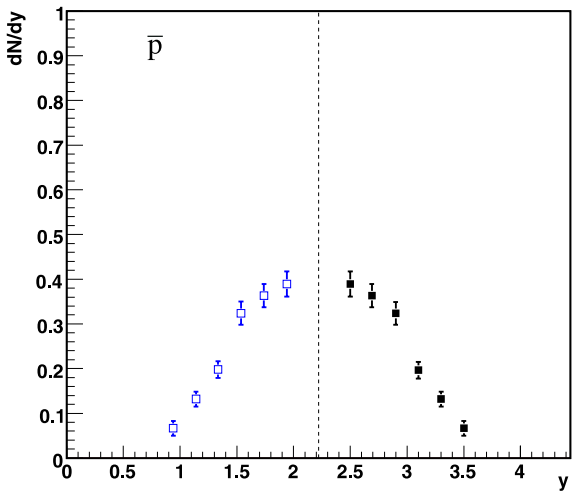

Fig. 6. Rapidity distribution of $\overline{p}$ in central Pb+Pb collisions at 40 A GeV. The *full symbols* indicate measured values, while the *open symbols* are reflected around midrapidity (*dotted line*)

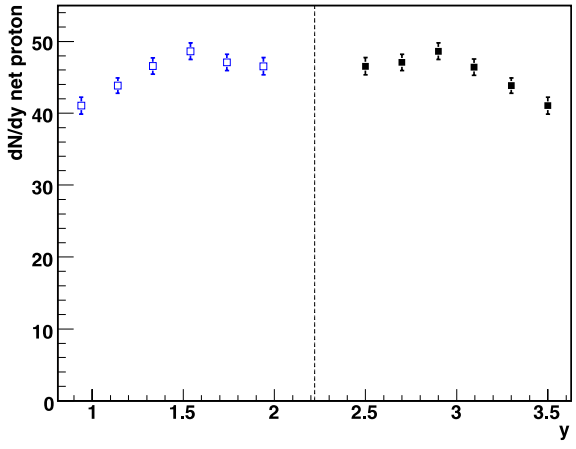

Fig. 7. Net proton distribution in central Pb+Pb collisions at 40 A GeV. The *full symbols* indicate measured values, while the *open symbols* are reflected around midrapidity (*dotted line*)

p and $\overline{p}$ is observed in central Pb+Pb collisions within the measured SPS energy range.

Preliminary results for the rapidity distributions of p and $\overline{p}$ at 40 A GeV were presented. They are consistent with the results at the highest SPS energy of $\sqrt{s_{NN}} = 17$ GeV. To complete the energy scan program of the NA49 experiment the rapidity spectra of p and $\overline{p}$ at all SPS energies need to be analysed.

Acknowledgements. This work was supported by the US Department of Energy Grant DE-FG03-97ER41020/A000, the Bundesministerium fur Bildung und Forshchung, Germany (06F137), the Virtual Institute VI-146 of Helmholtz Gemeinschaft, Germany, the Polish State Committee for Scientific Research (1 P03B 097 29, 1 P03B 121 29, 2 P03B 04123), the Hungarian Scientific Research Foundation (T032648, T032293, T043514), the Hungarian National Science Fundation, OTKA, (F034707), the Polish-German Fundatin, the Korea Research

Foundation Grant (KRF-2003-070-C00015) and the Bulgarian National Science Fund (Ph-09/05).

References

1. BRAHMS Collaboration, I.G. Bearden et al., Phys. Rev. Lett. **93**, 102 301 (2004)
2. NA49 Collaboration, H. Appelshäuser et al., Phys. Rev. Lett. **82**, 2471 (1999)
3. E917 Collaboration, B.B. Back et al., Phys. Rev. Lett. **86**, 1970 (2001)
4. E877 Collaboration, J. Barette et al., Phys. Rev. C. **62**, 024 901 (2000)
5. E802 Collaboration, L. Ahle et al., Phys. Rev. C. **60**, 064 901 (1999)
6. NA49 Collaboration, S.V. Afanasiev et al., Nucl. Instrum. Methods A **430**, 210 (1999)
7. NA49 Collaboration, S.V. Afanasiev et al., Phys. Rev. C **73**, 044 910 (2006)